

## Gamma-ray Multiplicities and Fission Modes in $^{208}\text{Pb}(^{18}\text{O}, f)$

G. G. Chubarian, M. G. Itkis<sup>a</sup>, N. A. Kondratiev<sup>a</sup>, E. M. Kozulin<sup>a</sup>, V. V. Pashkevich<sup>b</sup>, I. V. Pokrovsky<sup>a</sup>,  
A. Ya. Rusanov<sup>c</sup>, V. S. Salamatin<sup>a</sup> and R. P. Schmitt

<sup>a</sup>*Flerov Laboratory of Nuclear Reactions, JINR, 141980, Dubna, Russia*

<sup>b</sup>*Bogoliubov Laboratory of Theoretical Physics, JINR, 141980, Dubna, Russia*

<sup>c</sup>*Institute of Nuclear Physics of the National Nuclear Center of Kazakhstan, 480082, Alma-Ata, Kazakhstan*

A few years ago we started series of experiments to meticulously investigate the properties of low energy fission of the neutron deficient Th isotopes. The investigation of the fission cross sections and fission fragment mass-energy distributions (MED) of  $^{220,224,226}\text{Th}$  and  $^{220}\text{Ra}$  were presented in [1]. The new, multicomponent decomposition method of mass distributions was introduced in [2]. Recently, based on this method a detailed analysis of fission fragment mass distributions of  $^{226}\text{Th}$  isotopes was performed in [3]. As a result of multicomponent analysis of MED's four distinct fission modes were found. According to [4] these are, symmetric mode - S and three asymmetric modes, standard-1 (S1), standard-2 (S2), and standard-3 (S3). Earlier it was found that fission modality exhibits itself not only in the properties of MED's, but also in fission fragment angular distributions [5], post-fission neutron multiplicities  $\nu_{\text{post}}$  and their distributions [6]. In this work we will show that the phenomenon of multimodal fission also manifests itself in the  $\gamma$ -ray multiplicities ( $M_\gamma$ ) from fission fragments of the neutron deficient  $^{226}\text{Th}$  isotope.

Measurements of the  $\gamma$ -ray multiplicities in coincidence with the fission fragments in  $^{18}\text{O} + ^{208}\text{Pb}$  reaction at  $E_{\text{lab}}(^{18}\text{O}) = 78, 90, 117, 144,$  and  $198$  MeV will be discussed in the present work. Experiments were mainly conducted on

the K500 superconducting Cyclotron at Texas A&M University Cyclotron Institute with the exception of the reaction with the lowest beam energy of 78 MeV, which was carried out on the Tandem at LNS in Catania (Italy) [1].

The typical fission fragments MED's are shown in Fig. 1a-f At  $E_{\text{lab}} = 78$  MeV in mass distributions (MD) the asymmetric component in fission is clearly visible (Fig. 1a). It tends to have a higher total kinetic energy  $E_K$  for the mass range  $M_H > 125$  (Fig. 1c). In the mass range  $M_H = 130-134$  a well defined peak can be observed in dispersion of total kinetic energy as a function of mass  $\sigma_E^2(M)$  (Fig. 1e). In the same figure, for the energy  $E_{\text{lab}} = 78$  MeV the decomposition of MED on S, S2, and S1+S3 modes done within method [4] is shown. For the energy  $E_{\text{lab}} = 144$  MeV MED's are completely different. Single Gaussian shape of the MD, and parabolic shapes of  $E_K(M)$  and  $\sigma_E^2(M)$  testify to the disappearance of shell effects.

At  $E_{\text{lab}} = 78$  MeV the compound system is emitting approximately 1.5 pre-fission neutron  $\langle \nu_{\text{pre}} \rangle$  [7]. This means that at the scission point we will have compound nuclei close to  $^{224}\text{Th}$  with approximately 13 MeV less excitation energy. There are no direct experimental results on  $\langle \nu_{\text{pre}} \rangle$  for the same reaction at  $E_{\text{lab}} = 144$  MeV, but for a close reaction  $^{16}\text{O} + ^{208}\text{Pb}$  at  $E^* = 87$  MeV the number of pre-scission neutrons  $\langle \nu_{\text{pre}} \rangle \approx 4$  [8]. Then at the scission point we will

have  $^{222}\text{Th}$ . Below it will be shown that these circumstances do not affect the analysis and the interpretation of the experimental results.

In Fig. 1 g-j the  $\gamma$ -ray multiplicities  $M_\gamma(M)$  and their relative energies  $E_\gamma(M)$  as a function of fission fragment masses are shown. In the presented distributions significant differences may be noticed in the structures of  $M_\gamma(M)$  distributions at different beam energies. For the lowest beam energy  $E_{\text{lab}} = 78$  MeV, in

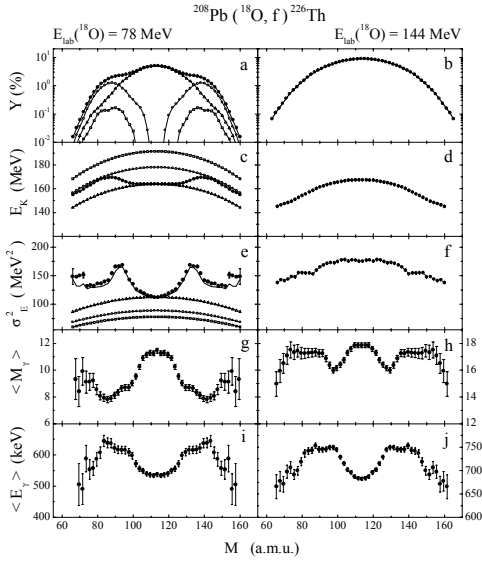


**Figure 1:** From top to bottom: Experimental yields  $Y$  of fission fragment masses (solid symbols) obtained at beam energies  $E_{\text{lab}} = 78$  and  $144$  MeV and results of decomposition (open symbols). The triangles correspond to the symmetric mode  $S$ , the circles - to mode  $S2$ , squares - to modes  $S1+S3$  (see text). Distributions of the total kinetic energy  $E_K(M)$  a function of fission fragment mass and its decomposition (the same designations). Dependence of the variance  $\sigma_E^2(M)$  of the fission fragment total kinetic energy on the mass, its decomposition and description (the solid curve). Smooth lines through the data points are for guidance only. For  $E_{\text{lab}} = 144$  MeV only  $S$  mode is realized. Gamma-ray multiplicities  $M_\gamma(M)$  and their relative energies  $E_\gamma(M)$  as a function of fission fragment masses.

the  $M_\gamma(M)$  distributions (Fig. 1g) three group of masses can be clearly noticed: first, around the

symmetric fission -  $M=(A/2)\pm 8$  with high  $\langle M_\gamma \rangle \approx \text{const} \approx 11.4$ , second with the local minimum at  $M_H = 128-130$ , and third with the lowest  $\langle M_\gamma \rangle \approx 8$  for the masses around  $M_H = 140$ . At the beam energy  $E_{\text{lab}} = 144$  MeV  $M_\gamma(M)$  distribution (Fig. 1h) still have a structure. There is a valley with a minimum at  $M_H \approx 128-130$ , but the second minimum around  $M_H \approx 140$  is transformed into a wide plateau with almost the same  $\langle M_\gamma \rangle$  value as for the symmetric part. In the  $E_\gamma(M)$  distributions (Fig. 1 i-j) situation is reversed. For intermediate beam energies  $E_{\text{lab}} = 90, 117$  MeV a smooth transition of structural peculiarities for lowest  $E_{\text{lab}} = 78$  MeV to higher  $E_{\text{lab}} = 144$  MeV beam energies is observed. At  $E_{\text{lab}} = 144$  MeV and  $E_{\text{lab}} = 198.5$  MeV the structures of  $M_\gamma(M)$  are very similar.

Gamma-rays are emitted from the fission fragments after evaporation of  $v_{\text{post}}$  at the very last stage of their de-excitation. At this point the internal structure of fission fragments is very important. If the number of nucleons in the final fragment is close to the magic numbers, for example  $Z_H \approx 50$ ,  $N_H \approx 82$  or  $N_L \approx 50$ , then the  $\gamma$ -ray cascade will reflect the structure of the nuclear states peculiar to near magic nuclei. These nuclei have minimal densities of quasi-particle and rotational excited states [9] and as a result the minimal value of  $\langle M_\gamma(M) \rangle$  will be observed. This will take place even if the initial fragment is heated and strongly deformed [10]. On the other hand during low energy fission at the scission point fragments can already be spherical [3,11]. In this case the densities of quasi-particle and rotational excited states are already minimal, therefore for these fragments ( $S1, S2$  modes)  $\langle M_\gamma(M) \rangle$  will be minimal. The set of calculated pre-scission deformations for cold and heated (up to  $E^* = 75$  MeV)  $^{224,222}\text{Th}$  nuclei is shown in Fig. 2. Nuclear shapes are

shown for the symmetric fission and ratios of masses 140/84 or 140/82, which correspond to the minimum of the fission valley on the potential energy surface for S2 mode, dominating the asymmetric mode at  $E_{\text{lab}} = 78$  MeV (Fig. 1). In the present experiment  $\langle M_i(M) \rangle$  from both fission fragments was measured, so only the summarized deformation at scission point may be discussed. As it is shown in Fig. 2 in the case of low energy fission the summarized deformation of both fragments for S2 mode ( $\langle M_H \rangle = 140$ ) is significantly less than for both heated nucleus or symmetric S mode of cold nucleus. On the other hand according to the modern ideas, fission fragments with the same mass can be formed in symmetric, as well in asymmetric valleys which is essential to those modes summarized deformations [1-4].

Generalizing all of the above, we can conclude that experimentally measured  $M_i$  may have two sources: primary fission fragments, if their structure of excited states is close to the final ones (asymmetric modes), and de-excited final fission fragments with their internal quasi-particle and rotational degrees of freedom, even if these fragments have the same nucleonic composition.

Now let us return back to Fig. 1. At the beam energy  $E_{\text{lab}} = 144$  MeV at a scission point all fission fragments are strongly heated and

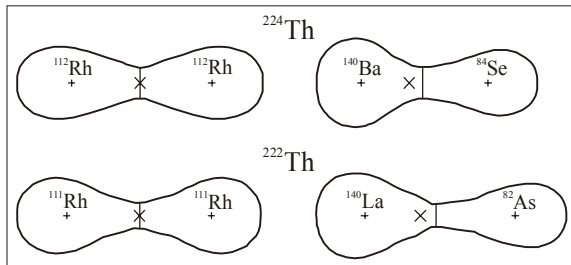


**Figure 2:** Theoretical calculations of pre-scission shapes for the “cold” fission of  $^{224}\text{Th}$  (upper part), and for the “hot” fission of  $^{222}\text{Th}$  (lower part).

deformed and their internal structure is insignificant. That is why the minima in  $M_i(M)$  at  $M_H = 128-130$  (and complementary to them) might be associated with the structure of fragments around the magic numbers  $Z_H \approx 50$ ,  $N_H \approx 80$  and  $N_L \approx 50$ . For all other masses there is no structure because they are far from the double-magic numbers. The minimum in  $M_i(M)$  around masses  $M_H = 128-130$  appears for all measured energies and is connected with the properties of the fission fragments in their final stage. Another minimum around  $M_H = 138-140$  at a lower beam energies reflects the existence of close to spherical shapes in heavy primary fragments near the scission point (S2 mode, Fig.2). In this case the light fragment is deformed. Nevertheless, the summarized deformation of both fragments is significantly less than for the same mass range with higher excitation energies. If we compare the structural peculiarities of the  $M_i(M)$  dependencies for both energies and also take into an account the overall increase of  $M_i$  with excitation energy:

$$\Delta M_i(M) = M_i(M) \Big|_{78} - (M_i(M) \Big|_{144} - 6.4) \quad (1)$$

we will get the “pure” input of the fission modes in the structure of the  $M_i(M)$  distributions. In Eq. (1) 6.4 is the difference of the  $\gamma$ -ray multiplicities for the symmetric S mode at the two beam energies. The difference of the  $\gamma$ -ray multiplicities  $\Delta M_i(M)$  is presented in Fig. 3. It was also approximated according to:

$$\Delta M_i(M) = \Delta M_i(M)^S(M)P^S + \dots + M_i^{S1+S2+S3}(M)P^{S1+S2+S3} \quad (2)$$

where  $M_i^i$  ( $i = S, S1 + S2 + S3$ ) is a  $\gamma$ -multiplicity for the mode  $i$ , and  $P^i$  is the relative probability of the given mode yield obtained

from decomposition of MED in Fig. 1. For S mode we assumed that  $M_\gamma^s$  does not depend on M and equals 11.4. From Fig. 3 it is clear that  $M_\gamma^s(M)$  is significantly higher than  $M_\gamma^{S1+S2+S3}(M)$ . Now if we assume that fission fragments are de-exciting through E2, transitions then the mean  $\gamma$ -ray multiplicities characterize their spin [10] and according to [9,12] depends directly on the deformation of fragments. From the data in Fig. 3 we can conclude that the mean value of the fragment spin at the scission point for S2 mode is substantially smaller than for S mode. This may be an evidence that the concept of the valley structure of the potential energy surface is a universal tool for an explanation of properties of a fissioning nucleus and fission fragments at the same time.

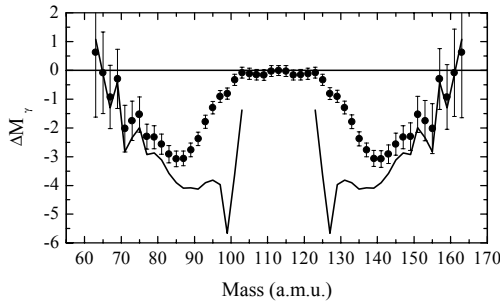


**Figure 3:** The difference of the  $\gamma$ -ray multiplicities (dots)  $\Delta M_\gamma(M)$  and its decomposition on S, S1+S2+S3 components in accordance with Eq. 2 (solid line), as a function of fission fragment mass.

Thus, for the first time in the  $M_\gamma(M)$  dependencies, for neutron deficient thorium isotopes, we were able to distinguish two components associated with primary and final (after the neutron evaporation) fission fragments, and show that at the scission point  $M_\gamma$

is extremely sensitive to symmetric and asymmetric modes of fission.

## References

- [1] G. G. Chubarian *et al.* in Proc. of the Fourth International. Conference on Dynamical Aspects of Nuclear Fission, (DANF'98), Casta-Papiernicka, Slovak Republic, October 1998, (World Scientific, Singapore, 2000), p.293; I. V. Pokrovsky *et al.*, Phys. Rev. C **60**, 041304 (1999).
- [2] S. I. Mulgin *et al.*, Phys. Lett. **B462**, 29 (1999).
- [3] I. V. Pokrovsky *et al.*, Phys. Rev. C **62**, 014615 (2000).
- [4] U. Brosa *et al.*, Phys. Rep. **197**, 167 (1990)
- [5] F. Steiper *et al.*, Nucl. Phys. **A563**, 282 (1993).
- [6] J. F. Wild *et al.*, Phys. Rev. C **41**, 640 (1990).
- [7] M. G. Itkis *et al.*, Nucl. Phys. **A654**, 870c (1999)
- [8] H. Rossner *et al.*, Phys. Rev. C **45**, 719 (1992).
- [9] A. V. Ignatyuk, Statistical Properties of Excited Atomic Nuclei (Energoatomizdat, Moscow, 1983), p. 71.
- [10] R. P. Schmitt *et al.*, Z. Phys. **A321**, 411 (1985); L. G. Moretto and R. P. Schmitt, Phys. Rev. C **21**, 204 (1980); R. P. Schmitt and A. J. Pacheco, Nucl. Phys. **A379**, 313 (1982).
- [11] Yu. V. Pyatkov *et al.*, Nucl. Phys., **A624**, 140 (1997).
- [12] J. O. Rasmussen *et al.*, Nucl. Phys. **A316**, 465 (1969); M. Zielinska-Pfabe and K. Dietrich, Phys. Lett. **B49**, 123 (1974).